

# Origin of magnetic fields in cataclysmic variables

Gordon P. Briggs<sup>1</sup>, Lilia Ferrario<sup>1</sup>, Christopher A. Tout<sup>1,2,3</sup>,  
Dayal T. Wickramasinghe<sup>1</sup>

<sup>1</sup>*Mathematical Sciences Institute, The Australian National University, ACT 0200, Australia*

<sup>2</sup>*Institute of Astronomy, The Observatories, Madingley Road, Cambridge CB3 0HA*

<sup>3</sup>*Monash Centre for Astrophysics, School of Physics and Astronomy, 10 College Walk, Monash University 3800, Australia*

Accepted. Received ; in original form

## ABSTRACT

In a series of recent papers it has been proposed that high field magnetic white dwarfs are the result of close binary interaction and merging. Population synthesis calculations have shown that the origin of isolated highly magnetic white dwarfs is consistent with the stellar merging hypothesis. In this picture the observed fields are caused by an  $\alpha$ – $\Omega$  dynamo driven by differential rotation. The strongest fields arise when the differential rotation equals the critical break up velocity and result from the merging of two stars (one of which has a degenerate core) during common envelope evolution or from the merging of two white dwarfs. We now synthesise a population of binary systems to investigate the hypothesis that the magnetic fields in the magnetic cataclysmic variables also originate during stellar interaction in the common envelope phase. Those systems that emerge from common envelope more tightly bound form the cataclysmic variables with the strongest magnetic fields. We vary the common envelope efficiency parameter and compare the results of our population syntheses with observations of magnetic cataclysmic variables. We find that common envelope interaction can explain the observed characteristics of these magnetic systems if the envelope ejection efficiency is low.

**Key words:** Stars: cataclysmic variables – stars: white dwarfs – stars: magnetic fields – stars: binaries.

## 1 Introduction

Cataclysmic variables (CVs) are close interacting binaries generally consisting of a low-mass main-sequence (MS) star transferring matter to the white dwarf (WD) primary via Roche lobe overflow (Warner 1995). In non-magnetic or weakly magnetic systems, which make up the majority of observed CVs, the hydrogen-rich material leaving the secondary star from the inner Lagrangian point forms an accretion disc around the white dwarf. It is estimated that some 20 – 25 per cent of all CVs host a magnetic white dwarf (MWDs, Wickramasinghe & Ferrario 2000; Ferrario et al. 2015a). These systems are the magnetic cataclysmic variables (MCVs). Among MCVs we have the strongly magnetic AM Herculis variables or polars. In polars the high magnetic field of the white dwarf can thread and channel the material from the secondary star directly from the ballistic stream to form magnetically confined accretion funnels, so preventing the formation of an accretion disc. In these systems the two stars are locked in synchronous rotation at the orbital period. The radiation from the accretion funnels (e.g. Ferrario & Wehrse 1999) and the cyclotron radiation from the shocks located at

the funnels’ footpoints of closed magnetic field lines dominate the emission of these systems from the X-rays to the infrared bands (e.g. Meggitt & Wickramasinghe 1982; Wickramasinghe & Ferrario 1988). Cyclotron and Zeeman spectroscopy and spectropolarimetry have revealed the presence of strong fields in the range of a few  $10^7$  –  $10^8$  G (see, e.g., Ferrario et al. 1992, 1993, 1996). Weaker fields of about  $10^6$  to  $3 \times 10^7$  G are found in the DQ Herculis variables or Intermediate Polars (IPs) where the white dwarf’s magnetic field cannot totally prevent the formation of an accretion disc (e.g. see Ferrario, Wickramasinghe & King 1993). In these systems the material is magnetically threaded from the inner regions of a truncated accretion disc and channelled on to the primary forming magnetically confined accretion curtains (Ferrario & Wickramasinghe 1993). In the IPs the white dwarf is not synchronously locked with the orbital period but is spun up to a spin period shorter than the orbital period of the system.

Liebert et al. (2005) noticed the enigmatic lack of MWDs from the 501 detached binaries consisting of a white dwarf with a non-degenerate companion found in the DR1 of the Sloan Digital Sky Survey (SDSS, York et al. 2000).

They also noticed that among the 169 MWDs known at the time, none had a non-degenerate detached companion. This was puzzling because such a pairing is very common among non-magnetic white dwarfs (see, e.g. Hurley, Tout & Pols 2002; Ferrario 2012). A similar study conducted on the much larger DR7 sample of SDSS detached binaries consisting of a white dwarf with a non-degenerate companion (Kleinman et al. 2013) led to the same conclusion (Liebert et al. 2015). Over the years, not a single survey conducted to ascertain the incidence of magnetism among white dwarfs has yielded a system consisting of a magnetic white dwarf with a non-degenerate companion (e.g., Schmidt et al. 2001; Kawka et al. 2007). It is this curious lack of pairing that led Tout et al. (2008) to propose that the existence of magnetic fields in white dwarfs is intimately connected to the duplicity of their progenitors and that they are the result of stellar interaction during common envelope evolution. In this picture, as the cores of the two stars approach each other, their orbital period decreases and the differential rotation that takes place in the convective common envelope generates a dynamo mechanism driven by various instabilities. Regős & Tout (1995) argued that it is this dynamo mechanism that is responsible for the transfer of energy and angular momentum from the orbit to the envelope which is eventually, all or in part, ejected.

Wickramasinghe, Tout & Ferrario (2014) have shown that strong magnetic fields in white dwarfs can be generated through an  $\alpha - \Omega$  dynamo during common envelope evolution where a weak seed poloidal field is wound up by differential rotation to create a strong toroidal field. However toroidal and poloidal fields are unstable on their own (Braithwaite 2009). Once the toroidal field reaches its maximum strength and differential rotation subsides the decay of toroidal field leads to the generation of a poloidal field with the two components stabilising each other and limiting field growth until they reach a final stable configuration. Thus, a poloidal seed field can be magnified during common envelope evolution by an amount that depends on the initial differential rotation but is independent of its initial strength. According to this scenario the closer the cores of the two stars are dragged at the end of common envelope evolution, before the envelope is ejected, the greater the differential rotation and thus the stronger the expected frozen-in magnetic field. If common envelope evolution leads to the merging of the cores the result is an isolated highly magnetic white dwarf. If the two stars do not coalesce they emerge from the common envelope as a close binary that evolves into a MCV. The viability of such model, in terms of incidence of magnetism among single white dwarfs and their mass and magnetic field distribution, have been shown by Briggs et al. (2015) and Briggs et al. (2018), henceforth referred to as paper I and paper II respectively.

In this paper we continue our studies of the origin of fields in MWDs to explain the parentage of MCVs. To this end we carry out a comprehensive population synthesis study of binaries for different common envelope efficiencies  $\alpha$ . We examine all paths that lead to a system consisting of a white dwarf with a low-mass companion star. We show that the observed properties of the MCVs are generally consistent with their fields originating through common envelope evolution for  $\alpha < 0.4$ .

## 2 Evolution and space density of MCVs

Observed MCVs consist of a white dwarf that accretes matter from a secondary star that has not gone through any significant nuclear evolution when the transfer of mass begins. The mass ratio of an MCV is given by  $q = M_{\text{sec}}/M_{\text{WD}} < 1$  where  $M_{\text{WD}}$  is the mass of the white dwarf primary and  $M_{\text{sec}}$  is the mass of the companion star. The mass accretion process in MCVs is relatively stable over long periods of time, although the polars suffer from high and low states of accretion. It is not known what sparks the change in accretion mode but, because polars do not have a reservoir of matter in an accretion disc, they can switch very quickly from high to low states. IPs have never been observed in low states of accretion. Stable mass transfer can be driven by nuclear-timescale expansion of the secondary (not generally applicable to MCVs) and/or by loss of angular momentum, driven by magnetic braking above the CV period gap (caused by the disrupted magnetic braking mechanism, see Spruit & Ritter 1983; Rappaport et al. 1983; Verbunt 1984) and gravitational radiation below the gap. Loss of angular momentum shrinks the orbit keeping the companion star filling its Roche lobe and so drives mass transfer. Therefore, as MCVs evolve, the orbital period diminishes until it reaches a minimum when the secondary star becomes a substellar-type object whose radius increases as further mass is lost. Systems that have reached the minimum period and have turned back to evolve toward longer periods are often called period bouncers (e.g. Patterson 1998)

The evolution of MCVs is expected to be similar to that of non-magnetic CVs. However, Li et al. (1994) have shown that angular momentum loss may not be as efficient in polars as it is in non-magnetic or weakly magnetic CVs in bringing the two stars together because the wind from the secondary star is trapped within the magnetosphere of the white dwarf. This phenomenon slows down the loss of angular momentum, reduces the mass transfer rate and leads to longer evolutionary timescales. This mechanism provides a simple explanation for the observed high incidence of magnetic systems among CVs (Araujo-Betancor et al. 2005). We show in Fig. 1 the period distribution of CVs and MCVs where the MCVs have been subdivided into polars and intermediate polars. The space density of CVs is not well known and, over the years, there has been some considerable disagreement between observations and theoretical predictions. The recent study of *Swift* X-ray spectra of an optically selected sample of nearby CVs conducted by Reis et al. (2013) has unveiled a number of very low emission X-ray systems. Hard X-ray surveys of the Galactic ridge have shown that a substantial amount of diffuse emission can be resolved into discrete low-luminosity sources. Because the MCVs are generally strong X-ray emitters, Munro et al. (2004) and Hong (2012) have propounded that IPs could be the main components of these low-luminosity hard X-ray sources.

Pretorius et al. (2013) have conducted a study of the X-ray flux-limited *ROSAT* Bright Survey (RBS) to determine the space density of MCVs. They assume that the 30 MCVs in the RBS are representative of the intrinsic population. They also allow for a 50 per cent high-state duty cycle for polars under the assumption that polars are below the RBS detection threshold while they are in low states of accretion. They find that the total space density of MCVs

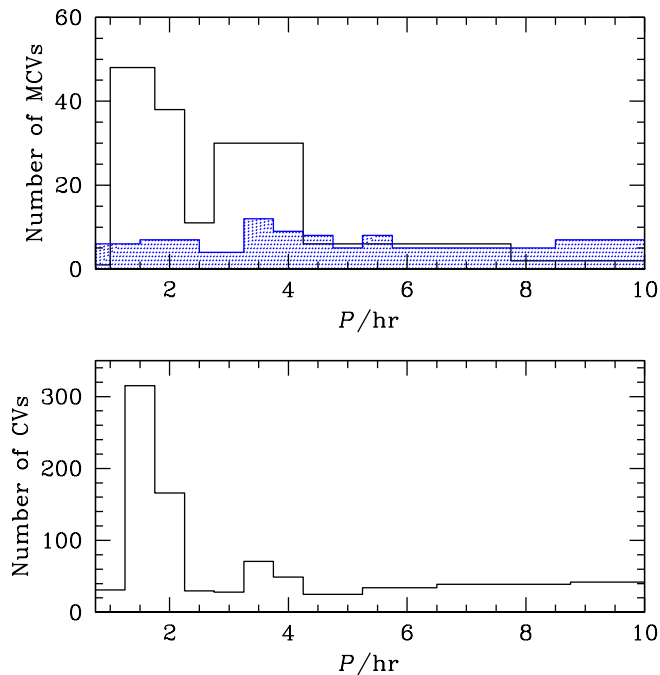


**Figure 1.** The orbital period distribution of MCVs (top) and CVs (bottom). The MCVs are subdivided into Polars (solid black line histogram) and IPs (shaded histogram). We have used the latest version (v7.20) of Ritter & Kolb’s (2003) CV catalogue to create this figure.

is  $1.3_{0.4}^{+0.6} \times 10^6 \text{ pc}^{-3}$  with about one IP per 200 000 stars in the solar neighbourhood. They conclude that IPs are indeed a possible explanation for most of the X-ray sources in the Galactic Centre. These new findings seem to suggest that the space density of CVs is somewhat larger than initially forecast and thus in closer agreement with theoretical expectations.

### 2.1 Where are the progenitors of the MCVs?

Liebert et al. (2005, 2015) asked, “Where are the magnetic white dwarfs with detached, non-degenerate companions?” This question is awaiting an answer and thus the progenitors of the MCVs still need to be identified. The proposal by Tout et al. (2008) that the existence of high magnetic fields in isolated and binary white dwarfs is related to their duplicity prior to common envelope evolution is gaining momentum. Observational support for the binary origin of magnetic fields in MCVs is also strengthening. Zorotovic et al. (2010) listed about 60 post common envelope binaries (PCEBs) from the SDSS and other surveys consisting of a white dwarf with an M-dwarf companion. The periods of these PCEBs range from about 0.08 to 20 d and the white dwarf effective temperatures in the range 7 500 to 60 000 K. According to current binary evolution theory, one third of these systems should lose angular momentum from their orbits by magnetic braking and gravitational radiation and are expected to come into contact within a Hubble time. However none of these 60 binaries contains a MWD, even if observations indicate that 20 to 25 per cent of all CVs harbour

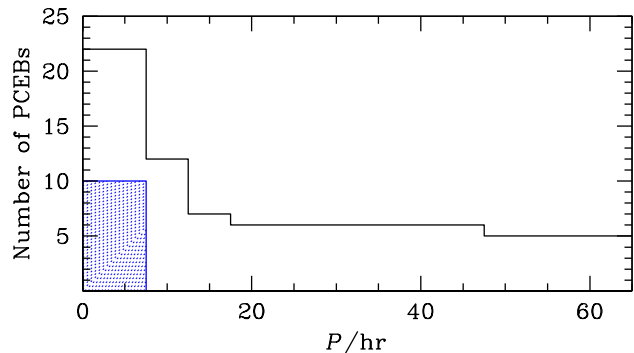


**Figure 2.** The orbital period distribution of PCEBs (solid black line histogram, Nebot Gómez-Morán et al. 2011) and PREPs (shaded histogram, Ferrario et al. 2015a).

one. This finding suggests that magnetic white dwarf primaries are only present in those binaries that are already interacting or are close to interaction. The magnetic systems originally known as Low-Accretion Polars (LARPS, Schwöpe et al. 2002; Ferrario, Wickramasinghe, & Schmidt 2005) have been proposed to be the progenitors of the polars. The first LARPS were discovered in the Hamburg/ESO Quasar Survey (HQS, Wisotzki et al. 1991) and then by the SDSS by virtue of their unusual colours arising from the presence of strong cyclotron harmonic features in the optical band together with a red excess owing to the presence of a low-mass red companion star. The MWDs in LARPS are generally quite cool ( $T_{\text{eff}} \lesssim 10\,000 \text{ K}$ ) and have low-mass MS companions which underfill their Roche lobes (e.g. Reimers et al. 1999; Schwöpe et al. 2002; Ferrario, Wickramasinghe, & Schmidt 2005; Parsons et al. 2013). The MWDs in these systems accrete mass from the wind of their companion at a rate substantially larger than in detached non-magnetic PCEBs (Parsons et al. 2013). Tout et al. (2008) suggested that LARPS could be pre-polars waiting for gravitational radiation to bring the stars close enough to each other to allow Roche lobe overflow to commence. These systems were renamed pre-polars (PREPs) by Schwöpe et al. (2009) to avoid confusion with polars in a low state of accretion. PREPs have orbital periods which are, on average, only marginally longer than those of polars. The ages of the white dwarfs in PREPs, as indicated by their effective temperatures, are generally above a billion years. The absence of PREPs with hot white dwarfs is puzzling but maybe still not alarming, if one considers the small number of PREPs currently known and the initial rapid cooling of white dwarfs. Thus, the hypothesis that the progenitors of MCVs are expected to emerge from common envelope when they are close to transferring mass via Roche Lobe overflow is well warranted. We show in Fig. 2 the period distribution of PCEBs and PREPs.

### 3 Population synthesis calculations

Each binary is assigned three initial parameters. These are the mass  $1.0 \leq M_1/M_{\odot} \leq 10.0$  of the primary star, the mass  $0.1 \leq M_2/M_{\odot} \leq 2.0$  of the secondary star, and the orbital period  $1 \leq P_0/\text{d} \leq 10\,000$  at the zero-age main sequence (ZAMS). We set the eccentricity to zero. We sam-

**Table 1.** We have indicated with  $N$  (second column) the fraction of PREPs for different efficiency parameters  $\alpha$  (first column) in a single generation of binaries. The other columns give the smallest and the largest progenitor masses and initial orbital periods.

$\alpha$	$N$ (per cent)	$M_{1\min}/M_{\odot}$	$M_{2\min}/M_{\odot}$	$M_{1\max}/M_{\odot}$	$M_{2\max}/M_{\odot}$	$P_{0\min}/\text{d}$	$P_{0\max}/\text{d}$
0.10	1.518	1.08	0.10	8.16	1.42	369.7	3144.0
0.15	1.672	1.08	0.10	8.16	1.42	293.3	2800.5
0.20	1.663	1.08	0.10	8.16	1.42	246.6	2354.3
0.25	1.213	1.08	0.10	8.16	1.36	207.3	2097.0
0.30	1.163	1.08	0.10	8.16	1.14	184.6	2221.9
0.50	0.808	1.08	0.10	8.16	0.58	123.2	2221.9
0.70	0.804	1.08	0.10	8.16	0.19	87.0	1867.9
0.80	0.859	1.08	0.10	8.16	0.13	69.1	1762.9

pled each parameter uniformly on a logarithmic scale with 200 divisions. This sampling gives a synthetic population of about 70 million binary systems. The actual number of binary systems is then calculated on the premise that  $M_1$  follows Salpeter’s mass function distribution (Salpeter 1955) and  $M_2$  is according to a flat mass ratio distribution with  $q \leq 1$ . The initial period distribution is assumed to be uniform in the logarithm.

We have used the rapid binary star evolution algorithm, BSE, developed by Hurley, Tout & Pols (2002), to evolve each binary system from the ZAMS to 9.5 Gyr (age for the Galactic Disc, Kilic et al. 2017). BSE is an extension of the single star evolution code written by Hurley, Pols & Tout (2000). It allows for stellar mass loss and interaction between the two stars such as mass transfer, Roche lobe overflow, common envelope evolution (Paczynski 1976), tidal interaction, supernova kicks, and angular momentum loss caused by gravitational radiation and magnetic braking.

In our modelling we have used the  $\alpha$  formalism for common envelope evolution. If  $\Delta E_{\text{orb}}$  is the change in orbital energy during the in-spiral phase and  $E_{\text{bind}}$  is the energy required to eject the envelope then

$$\Delta E_{\text{orb}} = \alpha E_{\text{bind}}.$$

Here  $\alpha$  is the common envelope efficiency parameter, ranging between 0.1 and 0.9, that takes into consideration the fact that the removal of the envelope is not totally efficient (see papers I and II for more details). The expression for the envelope binding energy contains another parameter  $\lambda$  which denotes the structure, or central condensation, of the envelope of the donor. This parameter is very uncertain and could vary by up to an order of magnitude (Tauris & Dewi 2001; Ivanova 2011). It depends on both the envelope structure and on the mass above which the envelope is expelled. In this work we follow Hurley, Tout & Pols (2002) and set  $\lambda = 0.5$ . A review on common envelope evolution and on the parameters that are used in its modelling can be found in Izzard et al. (2012).

Single star mass loss rates are described by Hurley, Pols & Tout (2000). In our calculations we have adopted  $\eta = 1.0$  for the Reimers’ mass-loss parameter, as outlined in paper I, and a stellar metallicity  $Z = 0.02$ .

Our theoretical sample of PCEBs consists of systems that (i) have undergone common envelope evolution, (ii) have a primary that evolves into a white dwarf, (iii) have a companion that remains largely unevolved and (iv) have a mass ratio  $q \leq 1$ . A subset of these systems come into contact over the age of the Galactic Disc and become clas-

sical CVs. Those systems with a white dwarf that develops a strong magnetic field become MCVs.

Of our sample of PCEBs, we then select the subset consisting of the PREPs (the progenitors of the MCVs). PREPs must fulfil two additional criteria: (i) the primary star must have a degenerate core before entering the last common envelope phase and (ii) no further core burning occurs. The reason for the first criterion is that a degenerate core is essential for a stellar magnetic field to persist, in a frozen-in state, after its formation. The reason for the second is that nuclear burning in the core would ignite convection that would destroy any frozen-in magnetic field. Systems that violate either criterion but come into contact over the age of the Galactic Disc are expected to evolve into classical non-magnetic CVs. We show in Table 1 the limits of the parameter space within which PREPs are formed. The minimum ZAMS masses of the systems that give rise to PREPs are listed in the columns with headings  $M_{1\min}$  and  $M_{2\min}$  and the maximum masses are under the headings  $M_{1\max}$ ,  $M_{2\max}$ . Minimum and maximum initial periods are in the columns under  $P_{0\min}$  and  $P_{0\max}$  respectively.

Once we have obtained our theoretical PREP sample, we assign a magnetic field  $B$  to each of their white dwarf primaries following the prescription described in paper II to model the field distribution of high field magnetic white dwarfs (HFMWDs). That is

$$B = B_0 \left( \frac{\Omega}{\Omega_{\text{crit}}} \right) \text{G}. \quad (1)$$

where  $\Omega$  is the orbital angular velocity and  $\Omega_{\text{crit}} = \sqrt{GM_{\text{WD}}/R_{\text{WD}}^3}$  is the break-up angular velocity of a white dwarf of mass  $M_{\text{WD}}$  and radius  $R_{\text{WD}}$ . The parameter  $B_0$  is a free parameter that was determined empirically in paper II, that is,  $B_0 = 1.35 \times 10^{10}$  G. The parameter  $B_0$  does not influence the shape of the field distribution which is only determined by  $\alpha$ . Lower (or higher)  $B_0$  shift the field distribution to lower (or higher) field strengths. Unlike HFMWDs, both stars emerge from common envelope evolution but on a much tighter orbit that allows them to come into contact within a Hubble time and appear as MCVs. Thus, white dwarfs in interacting binaries can only attain a fraction of the upper field strength of single white dwarfs and this is the reason why  $B_0$  must be determined through the modelling of HFMWDs (see paper II). Field strengths of MCVs are scaled down from the maximum by equation (1).



**Table 2.** The number of PCEBs born, the fraction of PREPs from PCEBs and of MCVs (magnetic systems already exchanging mass) from PREP as a function of the common envelope efficiency parameter  $\alpha$  over the age of the Galactic Disc. The number of PREPs is maximum close to  $\alpha = 0.15$  while the number of MCVs is maximum at  $\alpha = 0.10$ .

$\alpha$	Number of PCEBs	$\frac{\text{PREPs}}{\text{PCEBs}} \times 100$	$\frac{\text{MCV}}{\text{PREPS}} \times 100$
0.10	30517472	20.9	61.0
0.15	36099023	18.9	56.4
0.20	38666876	15.3	49.9
0.30	41197674	8.7	45.0
0.40	43654871	5.6	48.0
0.50	46289395	4.5	51.0
0.60	49010809	4.1	52.0
0.70	51888317	3.8	52.4
0.80	54664759	3.3	52.4

#### 4 Synthetic population statistics

We have time integrated each population, characterised by  $\alpha$ , to the Galactic Disc age under the assumption that the star formation rate is constant. We have listed in Table 2 the percentage by type of all binaries that emerge from common envelope over the age of the Galactic Disc.

Column 2 in Table 2 shows that while the number of PCEBs increases when  $\alpha$  increases, the percentage of PREPs (progenitors of the MCVs) decreases. This is because as  $\alpha$  increases the envelope’s clearance efficiency increases causing the two stars to emerge from common envelope at wider separations and thus less likely to become PREPs and thence MCVs. On the other hand, the overall number of PCEBs increases because stellar merging events become rarer at high  $\alpha$ , as shown in paper I. Fewer merging events are also responsible for the high incidence of systems with low mass He white dwarfs (He WDs) whose ZAMS progenitors were born at short orbital periods and entered common envelope evolution when the primary star became a Hertzsprung gap or a red giant branch (RGB) star. At larger initial orbital periods common envelope evolution may occur on the asymptotic giant branch (AGB). However as  $\alpha$  increases only stars in those systems that harbour massive enough white dwarfs can come sufficiently close to each other to allow stable mass transfer to occur within the age of the Galactic Disc (see section 4.2.3). In contrast, at low  $\alpha$  the clearance efficiency is low and so there is a longer time for the envelope to exert a drag force on the orbit. This results in (i) more merging events, (ii) tighter final orbits for all white dwarf masses and (iii) a larger number of systems coming into contact over the age of the Galactic Disc. Point (i) reduces the overall number of PCEBs while (ii) and (iii) increase the number of PREPs.

##### 4.1 Magnetic CV evolution examples

The evolutionary history of a binary system depends on the parameters that characterise it. The number of common envelope events can vary from one to several (Hurley, Tout & Pols 2002). Whether a classical CV becomes magnetic or not depends on the evolution before and after the common envelope. Here we give two typical examples of systems that evolve into a MCV. In the first the initially rather massive primary star evolves into a CO white

dwarf (CO WD) after common envelope evolution as a late AGB star. In the second example the primary evolves into a He white dwarf after common envelope evolution while ascending the RGB.

*Example 1:* Table 3 illustrates the evolution of a system that becomes a close binary after common envelope with  $\alpha = 0.1$ . The progenitors are a primary star (S1) of  $4.58 M_{\odot}$  and a secondary star (S2) of sub-solar mass  $0.230 M_{\odot}$ . At ZAMS the initial period is 2240 d with a separation of  $1220 R_{\odot}$ .

S1 evolves off the ZAMS and reaches the early AGB stage at 149 Myr having lost  $0.111 M_{\odot}$  on the way. After a further 1.02 Myr S1 has become a late AGB star. Further evolution brings the stars closer together at a separation of  $634 R_{\odot}$ . Soon after dynamically unstable Roche lobe overflow from S1 to S2 takes place and common envelope begins. At the end of the short period of common envelope evolution the two stars emerge with a separation of only  $1.05 R_{\odot}$  because of the large orbital angular momentum loss during this stage. The ejection of the envelope exposes the core of S1 that has now become a magnetic  $0.918 M_{\odot}$  CO WD. After a further 175 Myr the separation has further contracted to  $0.945 R_{\odot}$  via magnetic braking and gravitational radiation. Roche lobe overflow begins and the system becomes a bona fide mass-exchange MCV. During the MCV evolutionary phase the mass of the donor star, separation and orbital period steadily decrease until the mass of the companion star becomes too low to maintain hydrogen burning and S2 becomes a degenerate object. At this point separation and orbital period reach a minimum. Further evolution sees these two quantities increase again over time. At an age of 9500 Myr S2 has lost most of its mass and has become a  $0.037 M_{\odot}$  brown dwarf with the separation from its white dwarf primary increased to  $0.112 R_{\odot}$ .

*Example 2:* Table 4 shows the evolution of a second system that becomes a close binary after common envelope. This time we have  $\alpha = 0.4$ . The progenitors are a MS primary star (S1) of  $1.61 M_{\odot}$  and a secondary star (S2) of mass  $0.257 M_{\odot}$ . At ZAMS the initial period is 191 d and the separation  $172 R_{\odot}$ .

S1 evolves off the ZAMS through the Hertzsprung gap to reach the RGB after 2240 Myr having lost  $0.001 M_{\odot}$  on the way. Still on the RGB at 2340 Myr S1 has lost  $0.031 M_{\odot}$  and the separation has decreased to  $119 R_{\odot}$ . Roche lobe overflow from S1 to S2 and common envelope evolution begin. S1 emerges from common envelope as a magnetic He WD with a mass of  $0.386 M_{\odot}$ . The orbital separation has drastically decreased to  $1.02 R_{\odot}$ . S2 maintains its mass and remains an M-dwarf star. From this time onwards magnetic braking and gravitational radiation cause the orbit to shrink further until at 3390 Myr the separation is  $0.792 R_{\odot}$  and Roche lobe overflow commences. The system is now a MCV. Further evolution leads S2 to lose mass, owing to accretion on to S1, until, at 9500 Myr, S2 has become a brown dwarf of mass  $0.052 M_{\odot}$  and the separation is  $0.687 R_{\odot}$ .

##### 4.2 Property distributions of the synthetic population

We create our population of putative PREPs by integration over time from  $t = 0$  to  $t = 9.5$  Gyr. The star formation rate is taken to be constant over the age of the Galactic Disc. Whereas Table 1 shows the relative numbers of PREPs ob-

**Table 3.** Evolutionary history of an example binary system that becomes a MCV after common envelope evolution with  $\alpha = 0.1$ . Here CE = Common Envelope, RLO = Roche Lobe Overflow.

Stage	Time/Myr	$M_1/M_\odot$	$M_2/M_\odot$	$P/d$	$a/R_\odot$	$B/G$	Remarks
1	0.000	4.577	0.230	2244.627	1218.030	0.000E+00	ZAMS
2	128.515	4.577	0.230	2244.627	1218.030	0.000E+00	S1 is a Hertzsprung gap star
3	129.078	4.577	0.230	2245.210	1218.188	0.000E+00	S1 is a RGB star. Separation increases slightly.
4	129.445	4.574	0.230	2247.427	1218.790	0.000E+00	S1 starts core He burning. Some mass loss occurs.
5	149.930	4.466	0.230	2352.896	1247.059	0.000E+00	S1 is an AGB star. Further mass loss occurs.
6	150.947	4.390	0.230	2173.184	1176.321	0.000E+00	S1 is a late AGB star. Separation decreases significantly
7	150.989	4.364	0.230	861.296	633.510	0.000E+00	RLO & CE start. Separation decreases dramatically.
8	150.989	0.918	0.230	0.117	1.053	1.218E+07	S1 emerges from CE as a CO MWD and RLO ceases.
9	326.073	0.918	0.230	0.099	0.945	1.218E+07	Separation decreases and MCV phase starts
10	9 500.000	0.918	0.037	0.139	1.112	1.218E+07	Separation reaches a minimum between stages 9 and 10 and increases again. S2 is a brown dwarf.

**Table 4.** Evolutionary history of a second example binary system that becomes a MCV after common envelope with  $\alpha = 0.4$ .

Stage	Time/Myr	$M_1/M_\odot$	$M_2/M_\odot$	$P(d)$	$a/R_\odot$	$B/G$	Remarks
1	0.000	1.612	0.257	190.661	171.774	0.000E+00	ZAMS
2	2197.329	1.612	0.257	190.661	171.774	0.000E+00	S1 is a Hertzsprung gap star
3	2239.430	1.611	0.257	190.743	171.811	0.000E+00	S1 is a RGB star, loses mass. Separation increases slightly.
4	2343.048	1.580	0.257	110.351	118.629	0.000E+00	S1 loses more mass, separation decreases.
5	2343.048	0.386	0.257	0.149	1.020	3.577E+07	RLO & CE start. Separation decreases dramatically.
6	2343.048	0.386	0.257	0.149	1.020	3.577E+07	S1 emerges from CE as a He MWD and RLO ceases.
7	3389.278	0.386	0.257	0.102	0.792	3.577E+07	Separation decreases and MCV phase starts
8	9 500.000	0.386	0.052	0.100	0.687	3.577E+07	Separation reaches a minimum between stages 7 and 8 and increases again. S2 is a brown dwarf.

tained from a single generation of binaries, continuous star formation over the age of the Galactic Disc builds up a population of PCEBs, PREPs, CVs, and MCVs that, as birth time increases, favours systems with progressively higher mass primaries because lower mass primaries, especially in later generations, do not have enough time to evolve to the white dwarf stage.

#### 4.2.1 Period distribution

Figs 3 and 4 show the theoretical period distribution of the PREPs just before the beginning of Roche lobe overflow (RLOF) in a present day population formed over the age of the Galactic Disc for various  $\alpha$ . The contributions to the period distribution by white dwarf primaries of a certain type are depicted in Fig. 3 while the contributions to the period distribution by the secondaries of a given type are displayed in Fig. 4.

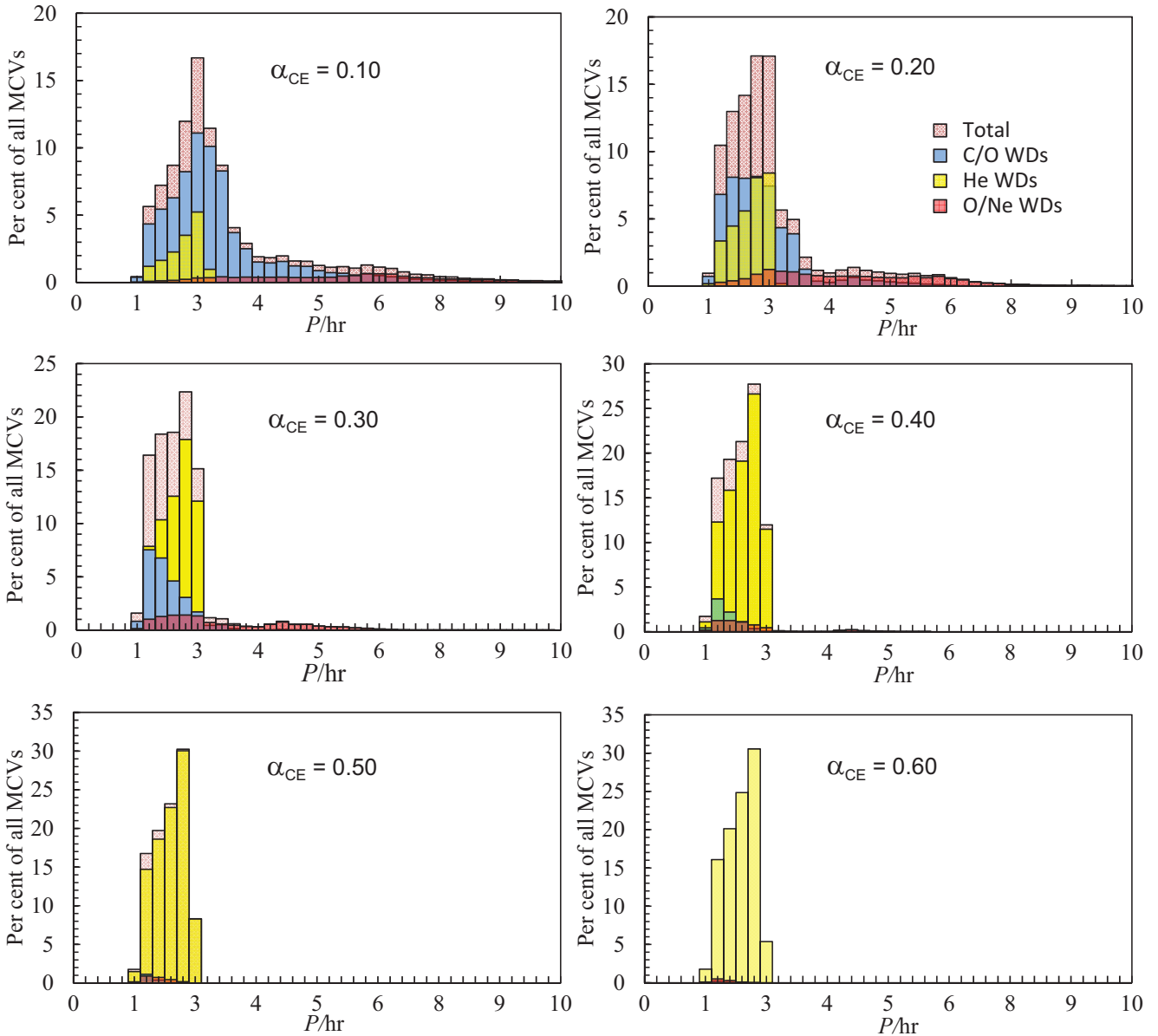
The period distribution peaks around 3 hr with a long tail extending to about 10 hr for low  $\alpha$ . We note that at low  $\alpha$  our synthetic population tends to have orbital periods clustering around the 1 to 4 hr region while at higher  $\alpha$  they are confined to the 1 to 3 hr region.

Fig. 3 shows that when  $\alpha = 0.1$  the main contributors to the whole range of periods are systems with CO WD primaries characterised by orbital periods from about 1 to 7 hr and a peak near 3 hr. Systems with He WDs are also present but are fewer and their periods are below 3 hr. Massive Oxygen-Neon white dwarf (ONe WD) primaries form a much smaller fraction of the distribution, as expected from Salpeter's initial mass function, but make some contribution to the full range of periods when  $\alpha < 0.4$ .

As  $\alpha$  increases the fraction of CO WD systems decreases until these all but disappear for  $\alpha > 0.5$  while the percentage of He WDs increases dramatically. For  $\alpha \geq 0.4$ , the orbital periods are always below 3 hr and He WD systems well and truly dominate the period distribution. For  $\alpha > 0.5$  the only systems that are predicted to exist are those with He WDs. The fraction of ONe WD systems reaches a maximum near  $\alpha = 0.2$  and then decreases.

We note that systems with He WDs tend to populate the lowest period range at all  $\alpha$ . These systems are generally characterised by initially lower-mass primaries, and thus lower-mass companions because  $q \leq 1$ , and shorter orbital periods and initiate common envelope evolution before helium ignition. Usually systems characterised by short initial periods are unlikely to survive at low  $\alpha$  because the stronger drag force exerted on the two stars during common envelope evolution causes them to merge.

Fig. 4 shows that most companions, particularly at shorter orbital periods, are low-mass deeply convective stars. More massive secondaries are generally found at longer periods for three reasons. First, longer orbital periods require high-mass white dwarfs to initiate stable mass transfer over the age of the Galactic Disc and these massive white dwarfs can have secondaries with masses all the way up to  $1.44 M_\odot$ , provided  $q \leq 1$ . Second, during common envelope evolution for a fixed primary initial mass and orbital period, systems with more massive secondaries have more orbital energy and so a smaller portion of this energy is necessary to eject the envelope. This leads to longer orbital periods. Third, for a fixed white dwarf mass, more massive secondaries fill their Roche lobes at longer orbital periods and so systems



**Figure 3.** Theoretical period distribution of magnetic systems just before they start RLOF for various  $\alpha$ 's. The period distribution of the primary white dwarf types is shown as the superimposed coloured categories. The total of the distribution is shown as the pink background histogram peaking around 2.8 to 3.0 hrs. This is to be compared with the observed distribution for PREPs in Fig. 2

with more massive companions are more likely to evolve into PREPs.

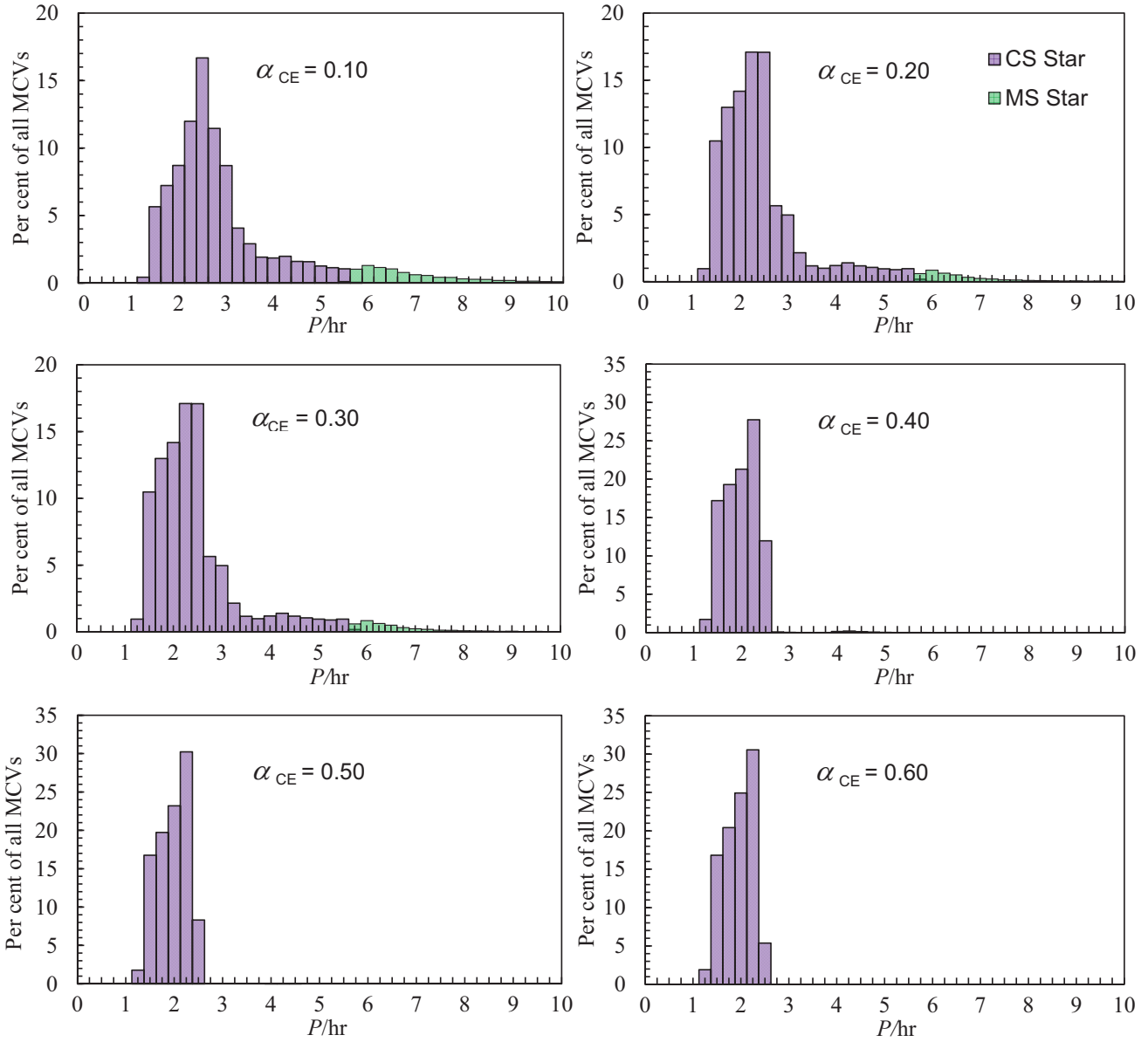
#### 4.2.2 Stellar pair distribution

Table 5 lists fractions of the various combinations of types of white dwarf primaries and secondary types just before RLOF commences. At low  $\alpha$  the predominant combination is a CO WD primary with a low-mass M-dwarf secondary. Second in abundance are systems comprised of a He WD with a low-mass M-dwarf secondary. Other combinations are also found but in much smaller numbers. At high  $\alpha$  the two major categories are swapped and those systems with He WD

primaries become the predominant type. The observed fraction of He WDs ( $f_{\text{He}}$ ) is generally low among classical CVs ( $f_{\text{He}} \lesssim 10$  per cent) and pre-CVs ( $f_{\text{He}} \lesssim 17 \pm 8$  per cent as shown by Zorotovic et al. (2011)). The results in Table 5 indicate that in order to reproduce the observed low fraction of He WDs our models need to be restricted to  $\alpha < 0.3$ .

#### 4.2.3 Mass distribution

Fig. 5 shows that all our models predict that, on average, longer orbital period systems contain CO WDs while shorter-period systems tend to have He WD primaries. At low  $\alpha$  the primaries are predominantly CO WDs with masses



**Figure 4.** Same as Fig.3 but with the secondary star types shown as the superimposed coloured categories. Both secondary star types are MS stars. The CS type is a deeply or fully convective MS star with  $M < 0.7 M_{\odot}$ .

**Table 5.** The fraction of the combinations of types of white dwarf primaries and secondary types just before RLOF commences for various  $\alpha$ . The stellar type CS is a deeply or fully convective low-mass MS star with  $M < 0.7 M_{\odot}$ .

$\alpha$	MCV progenitor pairs, fraction per cent					
	He WD/CS	CO WD/CS	ONe WD/CS	He WD/MS	CO WD/MS	ONe WD/MS
0.10	14.86	69.63	5.72	0.00	3.77	6.03
0.20	30.27	52.27	12.99	0.00	0.38	4.10
0.30	61.36	25.69	12.49	0.00	0.00	0.46
0.40	96.44	7.78	5.78	0.00	0.00	0.00
0.50	95.85	1.72	2.44	0.00	0.00	0.00
0.60	98.75	0.28	0.98	0.00	0.00	0.00
0.70	99.67	0.01	0.32	0.00	0.00	0.00
0.80	99.92	0.00	0.00	0.00	0.00	0.00



in the range  $0.5$  to  $1.1 M_{\odot}$  followed in lesser numbers by HeWDs with masses in the range  $0.4$  to  $0.5 M_{\odot}$  while ONe WDs, with masses in the range  $1.2$  to  $1.4 M_{\odot}$ , are rarer with their incidence reaching a maximum near  $\alpha = 0.2$ .

We note that there is a curious dip in the white dwarf mass distribution near  $M_{\text{WD}} = 0.8 M_{\odot}$  which widens as  $\alpha$  increases until all CO and ONe WDs disappear for  $\alpha > 0.5$ . This is because as  $\alpha$  increases, systems emerge from common envelope at progressively longer periods, because large  $\alpha$  means a high envelope clearance efficiency which leads to larger stellar separation at the end of the common envelope stage. However the longer the orbital period, the higher the white dwarf mass needs to be for stable mass transfer to commence. Thus the gap in the white dwarf mass distribution is caused by those systems that emerge from common envelope at large separations but with white dwarf primaries that are not massive enough to allow RLOF to take place. Another, albeit much narrower, gap occurs near  $0.5 M_{\odot}$  for all  $\alpha$  but becomes wider for  $\alpha \geq 0.2$ . This gap also persists until all CO and ONe WDs disappear at  $\alpha > 0.5$ . It divides systems with HeWDs primaries from those with CO WDs and is linked to whether the stars enter common envelope evolution on the RGB, and so produce a HeWD primary with  $M_{\text{WD}} \lesssim 0.5 M_{\odot}$ , or on the AGB, and so produce a CO WD primary with  $M_{\text{WD}} > 0.5 M_{\odot}$ .

Fig. 6 shows again that the secondaries are predominantly low-mass deeply or fully convective M-dwarf stars. The distribution has a broad peak around  $0.1$  to  $0.3 M_{\odot}$  at  $\alpha = 0.1$  to  $0.2$  with a long tail extending to  $1.2 M_{\odot}$ . As  $\alpha$  increases, the peak in the secondary mass distribution shifts to slightly lower masses (around  $0.1$  to  $0.25 M_{\odot}$ ) but the high-mass tail shrinks quite dramatically. At  $\alpha \geq 0.4$  the distribution is confined to secondary masses of less than about  $0.3 M_{\odot}$ . As already noted in section 4.2.1, the majority of these very low-mass donor stars belong to systems that underwent common envelope evolution during the Hertzsprung gap or RGB phases and thus have HeWD primaries with  $M_{\text{WD}} \lesssim 0.5 M_{\odot}$ . We also note that systems with low-mass secondaries ( $M_{\text{sec}} \lesssim 0.35 M_{\odot}$ ) remain detached for longer because magnetic braking is inefficient in these stars and gravitational radiation is the main source of loss of angular momentum.

#### 4.2.4 Magnetic field distribution

Fig. 7 shows the theoretical magnetic field distribution and the breakdown of the primary white dwarf types for our range of  $\alpha$ . The maximum field strength is a few  $10^8$  G and is found mostly in systems whose primary is a He WD. The reason for this is that systems that undergo common envelope evolution during the RGB evolution have shorter initial orbital periods and create very short period binaries with a highly magnetic white dwarf, as expected from equation (1).

The magnetic field distribution is dominated by systems with CO WD primaries when  $\alpha \leq 0.2$ . When  $\alpha \geq 0.4$  the field distribution becomes narrower and its peak shifts to higher field strengths. For  $\alpha \geq 0.5$  the field distribution only contains very highly magnetic He WD primaries with a peak near  $3.2 \times 10^8$  G. This shift to high fields is because those systems that go through common envelope evolution while their primaries are on the RGB merge for low  $\alpha$  but can

survive for high  $\alpha$  giving rise to very short orbital period systems with strongly magnetic, low-mass white dwarfs.

We note that the magnetic field distribution has a dip near  $8 \times 10^6$  G appearing at  $\alpha \geq 0.2$  and persisting until all CO and ONe WDs disappear from the distribution. This is reminiscent of the dip that we encountered in the white dwarf mass distribution (see 4.2.3) and has the same explanation. The similar behaviour is because the magnetic field strength is a function of white dwarf mass (by virtue of equations 1). The field dip is thus caused by the dearth of systems with white dwarf masses around  $0.8 M_{\odot}$  (see Fig. 5).

## 5 Comparison to observations

The optimal observational sample with which to compare our results would be that formed by the known magnetic PREPs. However, this sample is exceedingly small and observationally biased. To make things worse, not all PREPs have well determined parameters, such as masses and magnetic field strengths. Hence, for some of these studies we use the observed sample of MCVs, noting the following important points (i) the MCV sample is magnitude-limited, (ii) MCVs suffer from prolonged high and low states of accretion and (iii) MCVs include systems at all phases of evolution. Some of them began Roche lobe overflow billions of years ago while others have only recently begun mass exchange. Therefore, one should take such a comparison with some degree of caution particularly when we compare quantities that change over time, such as orbital periods and masses. When comparing masses we will also use the observed sample of non-magnetic Pre-CVs (Zorotovic et al. 2011).

The tables of Ferrario et al. (2015a) show that the observed orbital periods of MCVs are in the range  $1$  to  $10$  hr, masses are between about  $0.4$  and  $1.1 M_{\odot}$  and that the magnetic field distribution is relatively broad with a peak near  $3.2 \times 10^7$  G. A quick glance at Figs 3, 5 and 7 immediately reveals that models with  $\alpha > 0.3$  are all unable to reproduce the general characteristics expected from the progenitors of the observed population of MCVs and we elaborate on this in more details below. Generally, we see that models with  $\alpha > 0.3$  are not realistic and evolutionary effects cannot account for the large degree of discrepancy between theory and observations.

We begin our analysis with the magnetic field distribution. There is no evidence for field decay among MCVs (Ferrario et al. 2015a; Zhang et al. 2009) so we can assume that the magnetic field strength remains unchanged over the entire life of the magnetic binary.

We have used a Kolmogorov–Smirnov (K–S) test (Press et al. 1992) to compare the magnetic field distribution of the observed population with the theoretical results. This test establishes the likelihood that two samples are drawn from the same population by comparison of the cumulative distribution functions (CDFs) of the two data samples. The CDFs of the two distributions vary between zero and one and the test is on the maximum of the absolute difference  $D$  between the two CDFs. It gives the probability  $P$  that a random selection would produce a larger  $D$ . Five model CDFs for five different  $\alpha$ 's and the CDF for the known observed magnetic fields of 81 MCV systems are compared in Fig. 8.

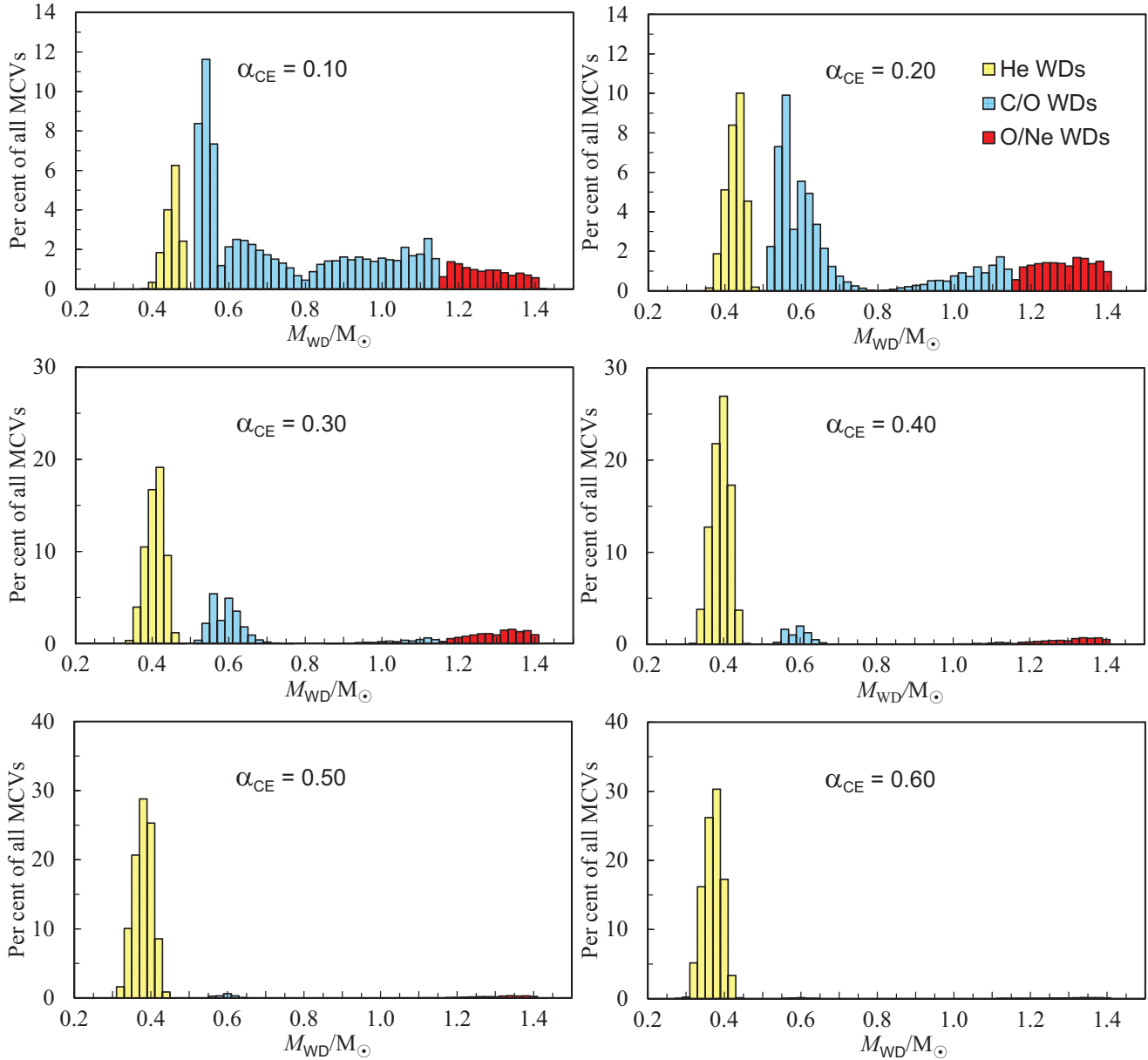


**Figure 5.** Theoretical mass distribution of the white dwarf primary star of magnetic systems just before they start RLOF for various  $\alpha$ . The distributions of the three white dwarf types are shown as three superimposed coloured categories.

The observed samples of MCVs and magnetic PREPs are very biased, particularly at the low and high ends of the magnetic field distribution. At low fields ( $B \lesssim 10$  MG) the observed radiation is dominated by the truncated accretion disc. In these low-field systems the photosphere of the white dwarf is never visible and Zeeman splitting cannot be used to determine field strengths. Nor can cyclotron lines be used to measure fields because they are too weak and invisible in the observed spectra. In the high field regime ( $B \gtrsim 100$  MG) mass accretion from the companion star is inhibited (Ferrario et al. 1989; Li et al. 1994) and so high field MCVs are very dim wind accretors often below the detection limits of most surveys (AR UMa Hoard et al. 2004). Be-

cause of these biases the observed samples in these regimes are far from complete and theoretical fits are unreliable. We therefore restrict our comparison between theory and observations to field strengths in the range 10 to 70 MG.

The results of the K-S test for our range of  $\alpha$  are displayed in Table 6 and show that the field distribution is a better match to the observations at low  $\alpha$ . The comparison of the magnetic field distribution between theory and observations is shown in Fig. 9 for  $\alpha = 0.1$ .

We stress that for  $\alpha > 0.3$  all the theoretical magnetic field distributions shown in Fig. 7 are very unrealistic because only very high field ( $B > 60$  MG) He WDs ( $M \lesssim 0.5 M_{\odot}$ ) are predicted to exist. This is contrary to ob-

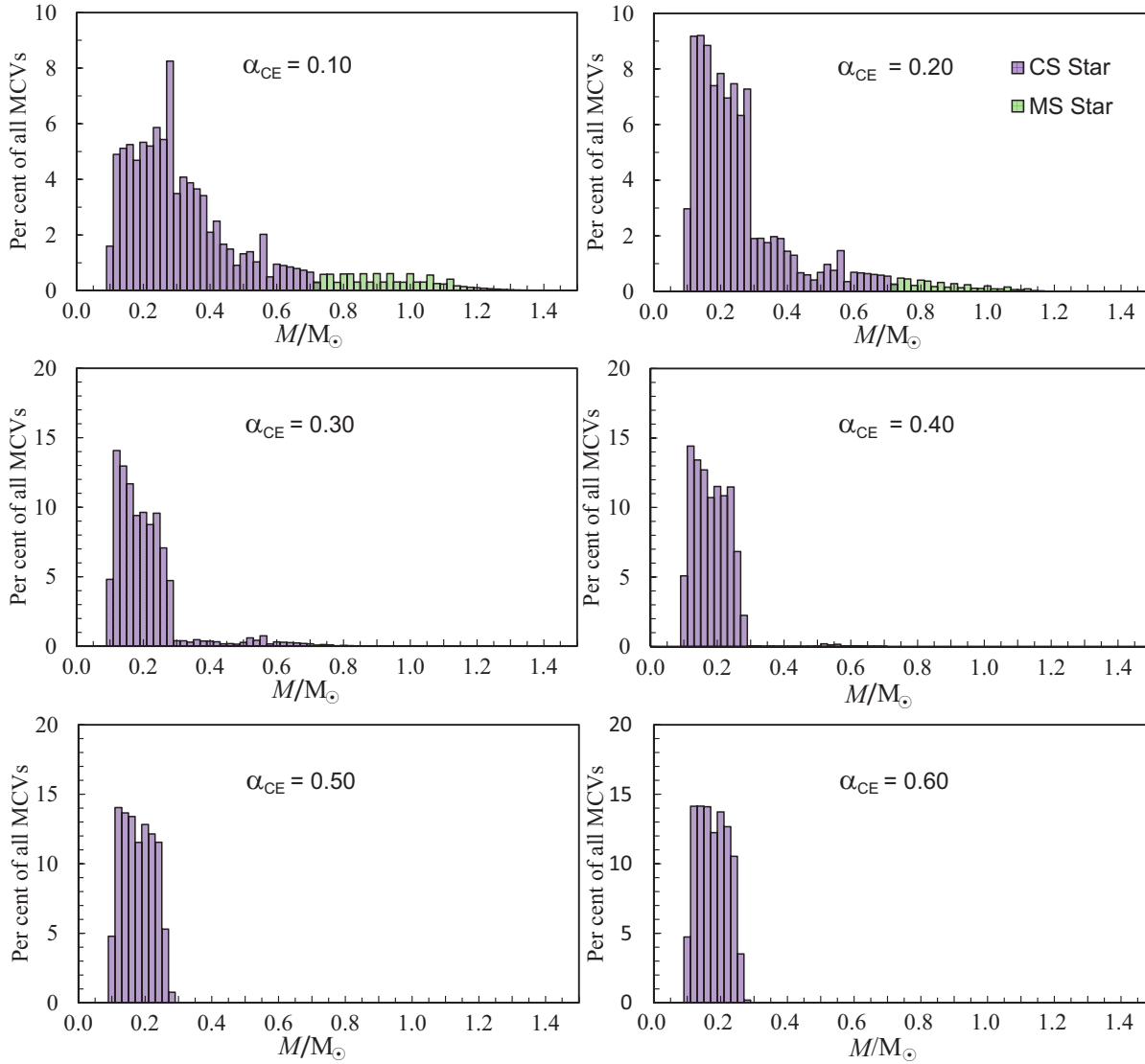


**Figure 6.** As in Fig 5 but for the secondary star types shown as the coloured categories. Both secondary star types are MS stars. The CS type is a deeply or fully convective MS star with  $M < 0.7 M_{\odot}$ .

servations that show that fields cover a much wider range of strengths (a few  $10^6$  to a few  $10^8$  G) and white dwarf masses ( $0.4$  to  $1.2 M_{\odot}$ ) as seen in Tables 2 and 3 of Ferrario et al. (2015a). We note here that a larger  $B_0$  with  $\alpha > 0.3$  is not a good fit because high  $\alpha$  models have a very narrow distribution of field strengths skewed to high fields. A larger  $B_0$  would only exacerbate this by pushing the distribution to even higher fields. If  $B_0$  were chosen at the lower end of the acceptable range found in paper II the field distribution would shift to lower fields and yield an aver-

age field strength closer to observations. However, because  $B_0$  can only shift the field distribution to lower (or higher) fields, the very narrow width of the distribution that characterises all our high  $\alpha$  models would not be corrected by readjusting  $B_0$ . We can therefore conclude that the  $B_0$  calibration carried out in paper II holds for the modelling of magnetic white dwarfs in binaries and supports our common envelope dynamo theory, according to which the fields of MCVs are scaled down, through equation (1), from the

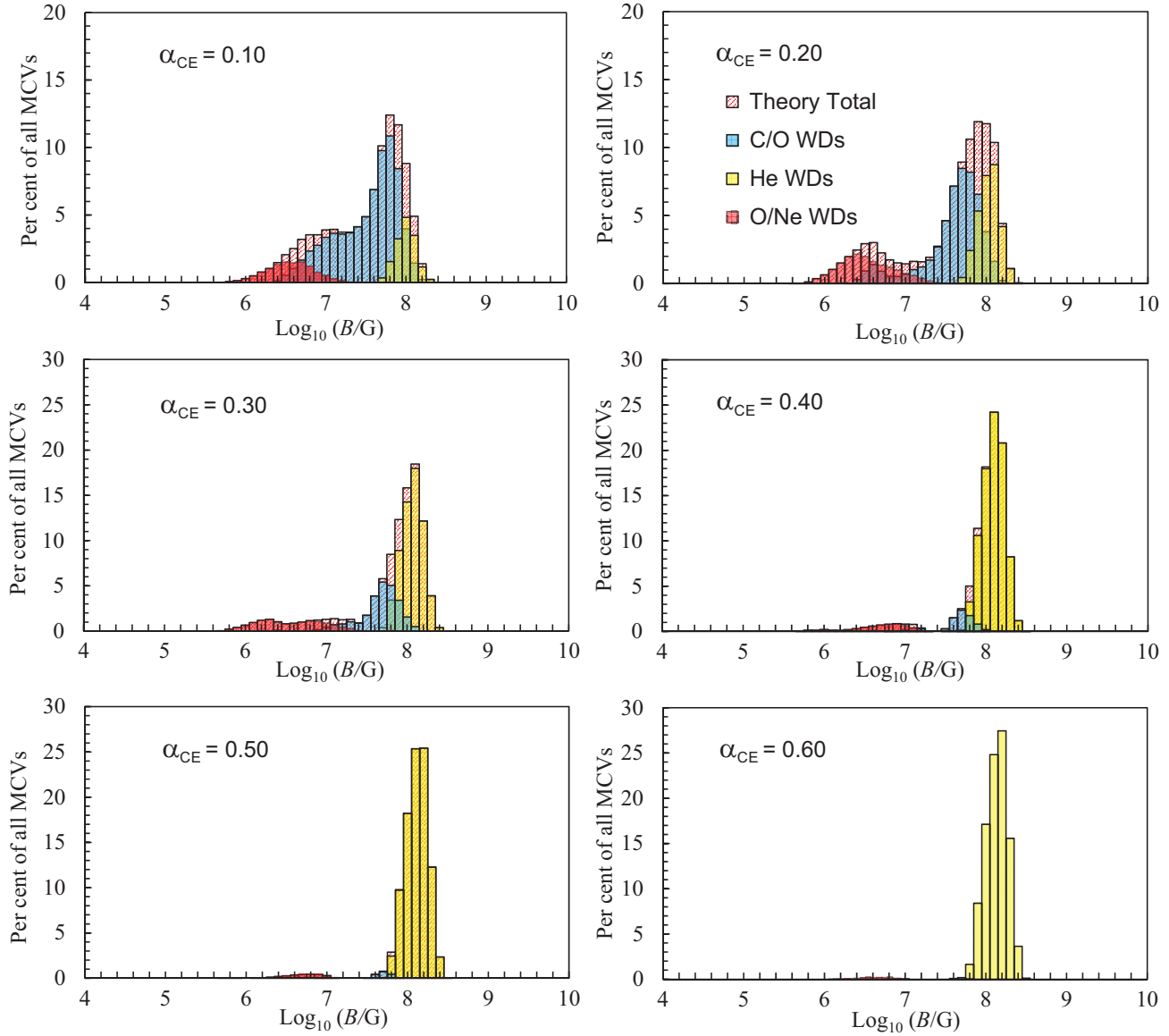


**Figure 7.** Pink shaded histogram: Total theoretical magnetic field distribution of the white dwarf primary stars in magnetic systems just before they start RLOF for the indicated  $\alpha$ . The histograms of the three types of white dwarfs making up the total theoretical magnetic field distribution are shown as the foreground coloured histograms. These three are made partially transparent so that details of the other histograms can be seen through them.

**Table 6.** Kolmogorov-Smirnov  $D$  statistic and probability  $P$  of the magnetic field distributions of the observed and synthetic populations of MCVs for a range of  $\alpha$ .

$\alpha$	$D$	$P$
0.10	0.17476	0.36069
0.15	0.19349	0.24632
0.20	0.25141	0.05845
0.30	0.22962	0.10500
0.40	0.26939	0.04298
0.50	0.35186	0.00429
0.60	0.38035	0.00006
0.70	0.61987	0.00000
0.80	0.94366	0.00000

maxima obtained during merging events that generate isolated HFMWDs.

We have performed a K-S study between the synthetic white dwarf mass distribution and that of white dwarf masses in MCVs taken from Ferrario et al. (2015a). In principle such a comparison can be justified if we make the usual assumption that the mass of the white dwarf does not grow in CVs because nova eruptions tend to expel all material that is accreted. However, we have found that the K-S test applied to the white dwarf masses of the theoretical and observed population of MCVs yields poor results, as shown in the second and third columns of Table 7. Such a conflict is not surprising because our assumption that the mass of the

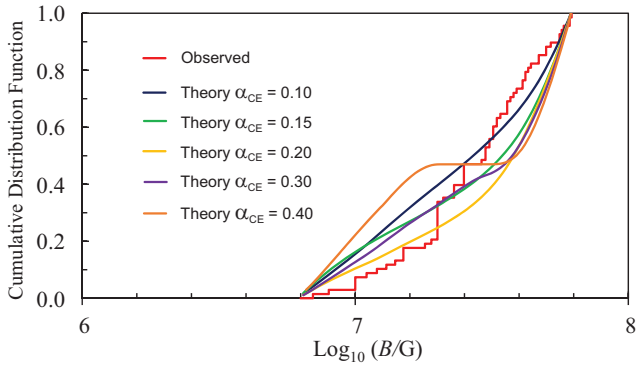


**Figure 8.** Theoretical cumulative distribution functions for the magnetic fields of MCV white dwarfs at RLOF for  $\alpha = 0.10, 0.15, 0.20, 0.30$  and  $0.40$  and the CDF of the observed magnetic field of 81 systems taken from Ferrario et al. (2015a)

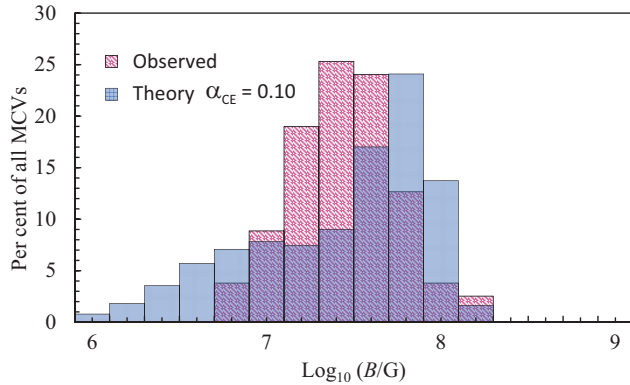


**Figure 9.** Comparison of the theoretical magnetic field strength for  $\alpha = 0.1$  and the observed magnetic field strength of the 81 MCVs taken from Ferrario et al. (2015a)

white dwarf does not grow because of nova eruptions may not be correct.

In this context, we note that Zorotovic et al. (2011) noticed a curious discrepancy in their observational data of CVs and Pre-CVs. That is, they found that the mean white dwarf mass in CVs ( $0.83 \pm 0.23 M_{\odot}$ ) significantly exceeds that of pre-CVs ( $0.67 \pm 0.21 M_{\odot}$ ) and they excluded that this difference could be caused by selection effects. The two possible solutions advanced by Zorotovic et al. (2011) were that either the mass of the white dwarf increases during CV evolution, or a short phase of thermal time-scale mass transfer comes before the formation of CVs during which the white dwarf acquires a substantial amount of mass via stable hydrogen burning on the surface of the white dwarf (as first suggested by Schenker et al. 2002). During this phase the system may appear as a super-soft X-ray source (Kahabka & van den Heuvel 1997). Using this assumption Wijnen et al. (2015) could build a large number of massive white dwarfs. However their model still created too many low-mass He WDs and too many evolved companion stars contrary to observations. Another possibility has recently been advanced by Zorotovic & Schreiber. (2017). In order to achieve a better agreement between their binary population synthesis models and observations of CVs they

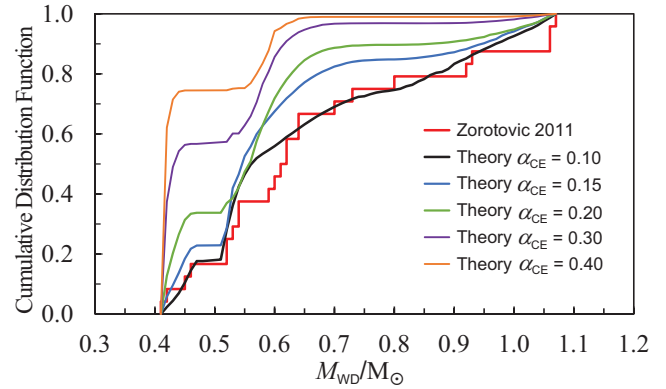


**Figure 10.** Cumulative Distribution Functions of the mass distributions for the observed pre-CV white dwarf masses taken from Zorotovic et al. (2011) and the theoretical distribution of the white dwarfs as the systems start RLOF for  $\alpha = 0.10, 0.15, 0.20, 0.30$  and  $0.40$ . The K-S statistics for this plot are shown in the fourth and fifth columns of table 7

adopted the ad-hoc mechanism proposed by Schreiber et al. (2016) which surmises the existence of additional angular momentum losses generated by mass transfer during the CV phase. Such losses are assumed to increase with decreasing white dwarf mass and would cause CVs with low-mass white dwarfs to merge and create an isolated white dwarf. By removing these merged systems from the synthetic CV sample the average white dwarf mass increases. Furthermore such a mechanism would explain the existence of isolated low-mass white dwarfs ( $M_{WD} < 0.5 M_{\odot}$ ) that constitute around 10 per cent of all single white dwarfs observed in the solar neighbourhood (e.g. Kepler et al. 2007).

Going back to our studies, if a comparison between white dwarf masses in MCVs and our synthetic population may not be meaningful, the next best sample to use for our K-S test is the observed white dwarf masses of pre-CVs (Zorotovic et al. 2011). We show in Fig. 10 the CDFs of the mass distributions for the observed sample and the theoretical distribution of the white dwarf masses at the beginning of RLOF for various  $\alpha$ . The results are reported in the fourth and fifth columns of Table 7 and show that the agreement between observations and theory is greatly improved. The comparison of the synthetic and observed Pre-CV white dwarf mass distribution is shown in Fig. 11 for the largest K-S probability at  $\alpha = 0.10$ . This suggests that the white dwarf mass distribution of the binary population in which primaries develop a magnetic field during common envelope evolution and later evolve to MCVs does not differ from that of the binary precursors of classical non-magnetic CVs.

We note that the Pre-CV observational sample shows a dearth of systems in the white dwarf mass distribution centred around  $0.8 M_{\odot}$ . This mass gap was already noted in the theoretical BSE models and the reasons for its existence were explained in section 4.2.3. The smaller size of this gap for models with  $\alpha \leq 0.2$  explains why we achieve a better fit with observations for  $\alpha = 0.1$ , as indicated by the K-S test.

If  $\alpha > 0.3$  the theoretical white dwarf mass distribution shown in Fig. 5 is very unrealistic because only He WDs ( $M < 0.5 M_{\odot}$ ) are predicted to exist by these models. This



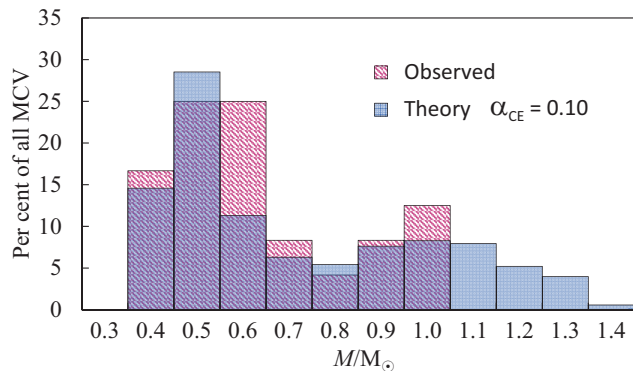


**Figure 11.** Comparison of the mass distributions for the observed pre-CV white dwarf masses taken from Zorotovic et al. (2011) and the theoretical mass distribution of the white dwarfs as the systems start RLOF for  $\alpha = 0.10$ .

**Table 7.** K–S  $D$  statistic and probability  $P$  of the white dwarf mass distributions of the observed MCVs listed by Ferrario et al. (2015a, second and third columns) and our synthetic populations for  $\alpha$  given in the first column. In the fourth and fifth columns we show the K–S results of the observed Pre-CV masses of Zorotovic et al. (2011) and our synthetic populations at the start of RLOF (fourth and fifth columns).

$\alpha$	$D$	$P$	$D$	$P$
0.10	0.37687	0.02023088	0.12954	0.95281557
0.15	0.49861	0.00064407	0.23478	0.34844783
0.20	0.56677	0.00006150	0.26010	0.23507547
0.30	0.62615	0.00000622	0.48014	0.18713800
0.40	0.69590	0.00000032	0.66148	0.00106500

is contrary to observations that show that masses cover the much wider range 0.4 to  $1.2M_{\odot}$  (see Tables 2 and 3 in Ferrario et al. 2015a).

Next, we look at the secondary mass distribution, keeping in mind that a comparison between our synthetic BSE mass sample and the observed secondary masses in MCVs is definitely not appropriate because secondary masses decrease over time as mass is transferred to the white dwarf. Nonetheless it may still be pertinent to use the observed Pre-CV sample to study and compare the overall characteristics of these samples so that we can, at the very least, discard some of the most extreme theoretical models.

Fig. 6 shows that if  $\alpha > 0.3$  then  $M_{\text{sec}} < 0.3M_{\odot}$ , which is inconsistent with observations of pre-CVs (see Zorotovic et al. 2011). Furthermore, we can see that when  $\alpha > 0.2$ , the decline towards higher masses becomes far too steep. This straightforward comparison seems again to indicate that models with  $\alpha > 0.3$  are very unrealistic and therefore low  $\alpha$  yields a better fit to observations.

## 6 Discussion and Conclusions

The origin of large-scale magnetic fields in stars is still a puzzling question (see Ferrario et al. 2015b). However, the results from recent surveys such as the SDSS (Kepler et al. 2013), BinaMIcS (Alecian et al. 2015) and MiMes (Wade et al. 2016) have provided us with a much

enlarged sample of magnetic stars that have allowed investigators to conduct studies like this one. There are two main competing scenarios to explain the existence of magnetic fields in white dwarfs. In 1981, Angel et al. proposed that the magnetic Ap and Bp stars are the most likely progenitors of the highly MWDs under the assumption of magnetic flux conservation (see also Tout et al. 2004; Wickramasinghe & Ferrario 2005).

The best clue so far on the origin of fields in white dwarfs (isolated and in binaries) has come from the study of their binary properties (Liebert et al. 2005, 2015), as outlined in section 2.1. This is why the proposal by Tout et al. (2008), that the origin of magnetic fields in white dwarfs is related to their duplicity and stellar interaction during common envelope evolution, is becoming more and more appealing.

We have extended our population synthesis study of binary systems carried out for papers I and II for the HFMDs to explain the origin of fields in the accreting white dwarfs in MCVs. Similarly to the investigations conducted in paper I and II, we have varied the common envelope efficiency parameter  $\alpha$  to investigate its effects on the resulting synthetic population of MCVs. We have shown that models with  $\alpha \geq 0.4$  are not able to reproduce the large range of white dwarf masses, field strengths, and secondary types and masses that are observed in MCVs and therefore models with  $\alpha < 0.4$  best represent the observed data. K–S tests conducted to compare our synthetic white dwarf mass and magnetic field distributions with the observed populations have given us some quantitative support in favour of models with  $\alpha < 0.4$ .

However, we need to stress again some of the shortcomings of our work and in particular those that arise from our comparison to observations. Many of the parameters (e.g., white dwarf mass, magnetic field, secondary star mass and type, orbital period) that characterise the Galactic populations of MCVs and PREPs and are needed for comparison studies are often hard to ascertain owing to evolutionary effects and observational biases that are difficult to disentangle. For instance, we mentioned in section 5 that magnetic white dwarfs in PREPs would be the best objects with which to compare our theoretical results and in particular the mass distribution, because mass is not contaminated by accretion processes. On the other hand there are far too few members of this population. The white dwarf mass distribution provided by the much larger sample of MCVs cannot be used either for comparison purposes because masses vary over time, owing to accretion and nova explosions. So we have used the sample provided by the non-magnetic Pre-CVs of Zorotovic et al. (2011).

The situation is somewhat ameliorated when we consider the magnetic field distribution because fields are not expected to change over time (see Ferrario et al. 2015a). However, the true magnetic field distribution of MCVs is not well known because it is plagued by observational biases. For example, at field strengths below a few  $10^7$  G most systems (the intermediate polars) have an accretion disc from which continuum emission and broad emission lines swamp the Zeeman and cyclotron features arising from the white dwarf surface and so hide those spectral signatures that are crucial to determine their field strengths. Very high field polars are also likely to be under-represented in the obser-

vational set because mass accretion from the companion star is impeded by the presence of strong fields (Ferrario et al. 1989; Li et al. 1998) making these systems very dim wind accretors.

Despite the limitations highlighted above, we have shown that the characteristics of the MCVs are generally consistent with those of a population of binaries that is born already in contact (exchanging mass) or close to contact, as first proposed by Tout et al. (2008). This finding is also in general agreement with the hypothesis that the binaries known as PREPs, where a MWD accretes matter from the wind of a low-mass companion, are the progenitors of the MCVs.

### Acknowledgements

GPB gratefully acknowledges receipt of an Australian Postgraduate Award. CAT thanks the Australian National University for supporting a visit as a Research Visitor of its Mathematical Sciences Institute, Monash University for support as a Kevin Westfold distinguished visitor and Churchill College for his fellowship.

### REFERENCES

- Alecian E. et al., 2015, in IAU Symp. 307, Meynet G., Georgy C., Groh J., Stee P., eds., Vol. 307, Geneva, Switzerland, pp. 330
- Angel J.R.P., Borra E.F., Landstreet J.D., 1981, ApJS, 45, 457
- Araujo-Betancor S., Gänsicke B.T., Long K.S., Beuermann K., de Martino D., Sion, E.M., Szkody P., 2005, ApJ, 622, 589
- Braithwaite J., 2009, MNRAS, 397, 763
- Briggs G.P., Ferrario L., Tout C.A., Wickramasinghe D.T., Hurley J.R., 2015, MNRAS, 447, 1713 (paper I)
- Briggs G.P., Ferrario L., Tout C.A., Wickramasinghe D.T., 2018, MNRAS, submitted (paper II)
- L Ferrario L., Wickramasinghe D.T., Bailey J.A., Hough J.H., Tuohy I.R., 1992, MNRAS, 256, 252
- Ferrario L., Bailey J., Wickramasinghe D.T., 1993, MNRAS 262, 285
- Ferrario L., Bailey J.A., Wickramasinghe D.T., 1996, MNRAS, 282, 218
- Ferrario L., Tuohy I.R., Wickramasinghe D.T., 1989, ApJ, 341, 327
- Ferrario L., Wehrse R., 1999, MNRAS, 310, 189
- Ferrario L., Wickramasinghe D.T., 1993, MNRAS, 265, 605
- Ferrario L., Wickramasinghe D.T., King A.R., 1993, MNRAS, 260, 149
- Ferrario L., Wickramasinghe D. T., Schmidt G. D., 2005, ASPC, 330, 411
- Ferrario L., 2012, MNRAS, 426, 2500
- Ferrario L., de Martino D., Gänsicke, B.T., 2015a, Space Science Review, 191, 111
- Ferrario L., Melatos A., Zrake J., 2015b, Space Science Review, 191, 77
- Hoard D. W., Schmidt Gary D., Szkody Paula, Ferrario Lilia, Fraser Oliver, Wolfe Michael A., Gänsicke B. T., 2004, 128, 1894
- Hong, J., 2012, MNRAS, 427, 1633
- Hurley J. R., Pols O. R., Tout C. A., 2000, MNRAS, 315, 543
- Hurley J. R., Tout C. A., Pols O. R., 2002, MNRAS, 329, 897
- Kahabka P., van den Heuvel E. P. J. 1997, ARA&A, 35, 69
- Ivanova N., 2011, ApJ, 730, 76
- Izzard R. G., Hall P. D., Tauris T. M., Tout C. A., 2012, IAUS, 283, 95
- Kawka A., Vennes S., Schmidt G.D., Wickramasinghe D.T., Koch R. 2007, ApJ, 654, 499
- Kepler, S. O., et al., 2007, MNRAS, 375, 1315
- Kepler, S.O., Pelisoli, I., Jordan, S. et al., 2013, MNRAS, 429, 2934
- Kilic, M., Munn, J.A., Harris, H.C., von Hippel, T., Liebert, J., Williams, K.A., Jeffery, E., DeGennaro, S., 2017, ApJ, 837, 2
- Kleinman S.J., Kepler S.O., Koester D., et al. 2013, ApJS, 204, 5
- Li J. K., Wu K. W., Wickramasinghe D. T., 1994, MNRAS, 268, L61
- Li J., Ferrario L., Wickramasinghe D. T., 1998, ApJ, 503, L151
- Liebert J. et al., 2005, AJ, 129, 2376
- Liebert J., Ferrario L., Wickramasinghe D.T., Smith P.S., 2015, ApJ, 804, 93
- Meggett S. M. A. & Wickramasinghe D. T., 1982, MNRAS, 198, 71
- Muno M.P., Baganoff F.K., Bautz M.W., Feigelson E.D., Garmire G.P., Morris M.R., Park S., Ricker G.R., Townsley L.K., 2004, ApJ, 613, 326
- Nebot Gómez-Morán A., Gänsicke B. T., Schreiber M. R., et al., 2011, A&A, 536, 43
- Parsons S.G., Marsh T.R., Gänsicke B.T., Schreiber M.R., Bours M.C.P., Dhillon V.S., Littlefair S.P., 2013, MNRAS 436, 241
- Patterson J., 1998, PASP, 110, 1132
- Paczynski B., 1976, in Eggleton P. P., Mitton S., Whelan J., eds, Proc. IAU Symp. 73, Structure and Evolution of Close Binary Systems, Reidel, Dordrecht, p. 75
- Press W. H., Teukolsky S. A., Vetterling W. T., Flannery B. P., 1992, p. 472, Numerical Recipes in Fortran 77. The Art of Scientific Computing, Cambridge Univ. Press, Cambridge
- Pretorius M.L., Knigge C., Schwobe A. D., 2013, MNRAS, 432, 570P
- Rappaport S., Verbunt F. Joss P. C., 1983, ApJ, 275, 713
- Reimers D., Hagen H.-J., Hopp U., 1999, A&A, 343, 157
- Reis R.C., Wheatley P.J., Gänsicke B.T., Osborne J.P., 2013, MNRAS, 430, 1994
- Regös E., Tout C.A., 1995, MNRAS, 273, 146
- Ritter H., Kolb U., 2003, A&A, 404, 301
- Salpeter E. E., 1955, ApJ, 121, 161
- Schenker K., King A. R., Kolb U., Wynn G. A., Zhang Z. 2002, MNRAS, 337, 1105
- Schmidt Gary D., Vennes S., Wickramasinghe D.T., Ferrario L. 2001, MNRAS, 328, 203
- Schreiber M. R., Zorotovic M., Wijnen T. P. G., 2016, MNRAS, 455, L16
- Schwobe A.D., Brunner H., Hambaryan V., Schwarz R.,

- 2002, in “The Physics of Cataclysmic Variables and Related Objects”, ASP Conf. Series, Eds: Gänsicke B.T., Beuermann K., Reinsch K., 261, 102
- Schwope A.D., Nebot Gomez-Moran A., Schreiber M.R., Gänsicke B.T., 2009, *A&A*, 500, 867
- Spruit H.C., Ritter H., *A&A*, 124, 267
- Tauris T. M., Dewi J. D. M., 2001, *A&A*, 369, 170
- Tout C.A., Wickramasinghe D.T., Ferrario L., 2004, *MNRAS*, 355, L13
- Tout C. A., Wickramasinghe D. T., Liebert J., Ferrario L., Pringle J. E., 2008, *MNRAS*, 387, 897
- Verbunt F., 1984, *MNRAS*, 209, 227
- Warner B., 1995, “Cataclysmic variable stars”, Cambridge: Cambridge University Press
- Wickramasinghe D. T., Ferrario L., 2000, *PASP*, 112, 873
- Wickramasinghe D. T., Ferrario L., 1988, *MNRAS*, 334, 412
- Wickramasinghe D. T., Ferrario L., 2005, *MNRAS*, 356, 615
- Wickramasinghe D. T., Tout C. A., Ferrario L., 2014, *MNRAS*, 437, 675
- Wijnen T. P. G., Zorotovic M., Schreiber M. R., 2015, *A&A*, 577, A143
- Wisotzki L., Reimers D., Wamsteker W., 1991, *A&A*, 247, L17
- York D.G., et al., 2000, *AJ*, 120, 1579
- Wade G.A., et al., 2016, *MNRAS*, 456, 2
- Zhang, C.M., Wickramasinghe D.T., Ferrario L., 2009, *MNRAS*, 397, 2208
- Zorotovic M., Schreiber M. R., Gänsicke B. T., Nebot Gómez-Morán A., 2010, *A&A*, 520, 86
- Zorotovic M., Schreiber M. R., Gänsicke B. T., 2011, *A&A*, 536, 42
- Zorotovic M., Schreiber M. R., 2017, *MNRAS*, 466, L63